Persistence length of the Debye-Hückel model of weakly charged flexible polyelectrolyte chains

Uwe Micka[1] and Kurt Kremer[1,2]
[1]*Institut für Festkörperforschung, Forschungszentrum Jülich, Postfach 1913, D-52425 Jülich, Federal Republic of Germany*
[2]*Max-Planck-Institut für Polymerforschung, D-55021 Mainz, Federal Republic of Germany**
(Received 20 December 1995)

We present simulations of the basic analytic model of weakly charged polyelectrolytes: monovalently charged monomers with Debye-Hückel interaction coupled by harmonic springs. Quantities such as the chain radii, bond lengths, structure factors, persistence lengths, and scaling properties were examined. The persistence length L_P shows a sublinear dependence on the screening length $r_D=1/\kappa$ ($L_P\sim\kappa^{-y}, y<1$) in strong contrast to all known analytical approaches which propose either $y=2$ or $y=1$. The observed exponent y varies as a function of κ and the bond length b. [S1063-651X(96)03308-9]

PACS number(s): 61.25.Hq, 36.20.−r, 87.15.He, 05.20.−y

I. INTRODUCTION

The theoretical understanding of polyelectrolytes is rather weak compared to that of neutral polymers [1]. The main reason is the occurrence of the long-ranged Coulomb interaction. The large number of degrees of freedom of the counterions and their fluctuations form another serious problem. Furthermore, the comparison between experiment and theory is often very difficult because of different regions of validity concerning the density of the solution. Scattering experiments need a certain contrast and therefore it is almost impossible to study extremely dilute solutions, which are the topic of most theories. Additionally, experiments as simulations face severe finite size effects in search for general asymptotic behavior. In such a situation, computer simulations have the important possibility to build a bridge between theory and experiment as they can test theoretical aspects as well as experimentally measurable quantities under well controllable conditions (see, e.g., [2]).

The aim of the present work is not to give a description of polyelectrolytes in solution that is as physical as possible but to test certain theoretical concepts for model systems. The question whether the theories of Odijk [3] and Skolnick and Fixmann [4] (for the rest of this paper referred to as OSF) remain valid for intrinsically flexible chains [5,6] or whether several variational ansatzes [7–9] give the right description is addressed in this work. Because we are looking for the advantages and shortcomings of the two treatments of the very same model, we employ exactly the same Hamiltonian as all the above papers. The polymers are modeled by bead-spring chains. Every neutral part in between two charges, which is supposed to be a random walk, is represented by a harmonic spring and the charged monomers interact via screened Coulombic interaction. The screening of the counterions is usually accounted for by the solution of the linearized Poisson equation, the Debye-Hückel (or Yukawa) potential V_{DH}. This, however, is known to be a rather crude approximation [10]. With $r_D=1/\kappa$ being the screening length the potential reads

$$V_{\mathrm{DH}}=\frac{q^2}{4\pi\epsilon\epsilon_0}\frac{\exp(-\kappa r)}{r}=\lambda_B k_B T\frac{\exp(-\kappa r)}{r}, \qquad (1)$$

where q is the charge per monomer and $\epsilon\epsilon_0$ is the dielectricity constant of the solvent. $\lambda_B=q^2/4\pi\epsilon\epsilon_0 k_B T$ is the Bjerrum length, which describes the strength of the bare Coulomb interaction. Therefore the present chains are given by the following Hamiltonian:

$$H=\sum_{i=1}^{N-1}\frac{3k_BT}{2b^2}(\vec{r}_i-\vec{r}_{i+1})^2+\sum_{i=2}^{N}\sum_{j=1}^{i-1}\lambda_B k_B T\frac{\exp(-\kappa r_{ij})}{r_{ij}}, \qquad (2)$$

with N being the number of beads, $r_{ij}=|\vec{r}_i-\vec{r}_j|$ the distance between two charges, q_i the charge of the ith bead, k_B the Boltzmann constant, and T the temperature. $b=\sqrt{\langle\vec{b}^2\rangle}$ ($\vec{b}$ bond vector; $\langle\vec{b}\rangle=\vec{0}$) is the expectation value of the end-to-end distance of a corresponding random walk, which is supposed to model a neutral Θ chain in between the charges with b^2 Kuhn steps. This also allows a comparison to experimental systems. All lengths are measured in units of such a Kuhn segment length. Some models use a continuous charge distribution. For large systems (and especially large and medium distances) there should be no difference between these approaches and our model. In this respect our model is nearer to experiments and therefore should be the choice.

In Sec. II the computational method and the calculated quantities are introduced in detail, followed by results concerning chain radii, bond stretching, and attempts to find scaling variables. In Sec. IV the scaling plots of our system are shown. A crossover from a blob pole behavior to the self-avoiding walk (SAW) regime is found. In Sec. V a more detailed test is employed to directly access the κ dependence of the persistence length by calculating the bond angle correlation including a careful analysis of finite size effects. To support these overall results, the chain structure factor is analyzed in Sec. VI. Similarities with recent computer simulations of strongly charged polyelectrolytes [10] are found. Finally, Sec. VII will give a short summary and outlook.

*Present address.

II. MODEL AND SIMULATION METHOD

As already noticed, the theoretical description is based on an underlying Θ chain, represented by the harmonic potentials between successive monovalently charged monomers. Those monomers interact via a Debye-Hückel potential leading to the Hamiltonian (2). For such a system with strongly fluctuating bond lengths, there is a natural need to equilibrate the short and long length scales as well as possible. To do so, we combine a velocity verlet molecular dynamics (MD) coupled to a heat bath with a Monte Carlo procedure (MC). For the Monte Carlo part the off-lattice pivot algorithm turned out to be the most efficient choice. The MD part is performed at constant temperature $k_BT=1.0\epsilon$ using the Langevin thermostat with damping constant $\gamma=1.0\tau^{-1}$ and time step 0.0125τ where τ is the characteristic time of the system [11]. We typically start with some 1000 MD steps to allow for initial bond stretching. Then the pivot procedure equilibrates the large scale structure (several 10 000 steps). Then MD mixed with rare pivot steps generates the final configurations. For comparison also simulations with fixed bond length were performed. In this case only the pivot algorithm is used. Systems embedded in three and in two dimensions were simulated. The latter was done to compare our results for the bond angle correlation function with those of Barrat and Joanny [12] . The equilibrium is defined by comparison of two extreme starting conformations: the random walk and the totally stretched state. The equilibrium is reached when both simulations produce the same values for several testing quantities such as the end-to-end distance R_{end}, the radius of gyration R_G, and the bond length b. The program uses the vector facilities of a CRAY YMP supercomputer and simulates 640 independent polyelectrolyte chains in parallel. (Only for $N=512$ the number of polymers was reduced to 320.) In a similar way the algorithm can be parallelized trivially. When equilibrium is reached, the quantities of interest are averaged over the 640 chains. Note that we have 640 truly independent states, giving true statistical errors of 4% only. For local quantities that allow for an intrachain average the statistics are even better.

The screening parameter κ was varied from $\kappa=0.001$ up to $\kappa=0.48$ (in extreme cases) giving a Debye screening length between 1000 and 2.083. This covers length scales smaller than the distance between two successive charges up to larger than the whole chain extension. The Bjerrum length is fixed to $\lambda_B=1$. The unit length is defined by the length of the Kuhn step of the underlying neutral random walks between the charges, which are modeled by the harmonic springs. Several values of the degree of polymerization N allow one to examine the finite size effects, which appear to be very strong and extremely relevant in experiments too (see Sec. V). By combining the different chain lengths with five values of the bond length b, the whole experimentally relevant range of molecular weights is covered. This fact points out that the comparison of our results (e.g., for the structure factor, see Sec. VI) with experimental data should be possible and allow some conclusions on the general validity of the Debye-Hückel approach. We use chain lengths $N=16$, 32, 64, 128, 256, and 512 and bond lengths $b=2$, 4, 8, 10, and 16. Taking into account the relation $N\sim R_{\mathrm{end}}^2$ for a random walk, our largest polymer consists of $(N-1=511)\times(b=16^2)=511\times256\approx131\,000$ monomers. Comparing this system to a NaPSS-PS block copolymer (molecular weight: $m_{\mathrm{NaPSS}}=221$ and $m_{\mathrm{PS}}=104$) we reach molecular weights beyond 13 000 000 g/mol, which is beyond experiment. Even for strongly charged chains our systems lie in the experimentally relevant region; e.g., a $N=512$ bead chain mapped on a NaPSS in water under the assumption that every third monomer is charged (which is shown to be reasonable by experiments—monomer size ≈2.5Å, $\lambda_B\approx7.14$Å—and very similar to our $b=2$ chains) models a molecular weight of at least 340 000 g/mol. All in all, we can cover the experimentally relevant parameter space by varying our parameters.

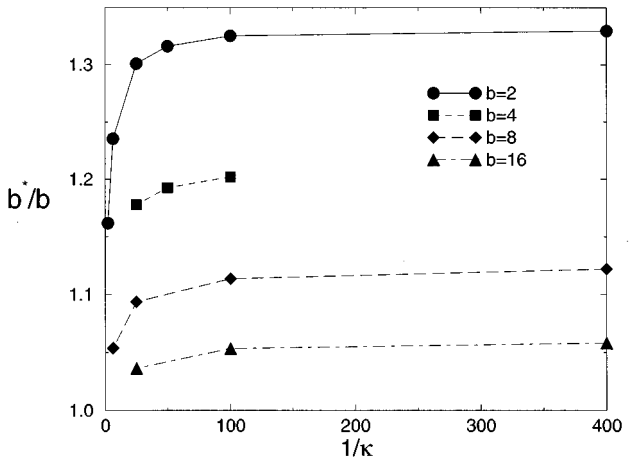

FIG. 1. Relative stretching of the bond length b as a function of $1/\kappa$ for $N=128$.

III. FIRST RESULTS

Due to the Coulomb repulsion of the charges, the springs between monomers become stretched. The usual assumption is that the chain structure inside a blob is not strongly affected by the Coulomb interaction. Figure 1 shows an example of the stretching as a function of κ. As expected, the smaller κ, the stronger is the elongation. With increasing bond length (reduced effective charge density) the relative stretching decreases for fixed κ. Taking all the data, the tendencies are unambiguous but no simple power law can be deduced. It is important to take care of finite size effects resulting from the free chain ends. Apart from these end monomers, the bond length distribution is flat.

A characteristic quantity for the shape of the chains is the ratio $r=R_{\mathrm{end}}^2/R_G^2$ as it sensibly measures the large scale stretching due to the Coulomb repulsion. Here $R_{\mathrm{end}}=\sqrt{(\vec{r}_N-\vec{r}_1)^2}$ is the end-to-end distance and $R_G=\sqrt{(1/N)\Sigma_{i=1}^{N}(\vec{r}_i-\vec{r}_{CM})^2}$ is the radius of gyration. For random walks this ratio equals 6 while for a totally stretched chain 12 is expected. A value around 6.3 is known for SAW. Figure 2 shows that beginning in a SAW regime the chains are stretched up to a value of 10. Even for extremely weakly screened systems ($r_D=1/\kappa$ > chain dimensions) the chains are not totally stretched. This is in accordance to recent simulational results of strongly charged polyelectrolytes [10]. Nevertheless in Sec. IV it is shown that these chains

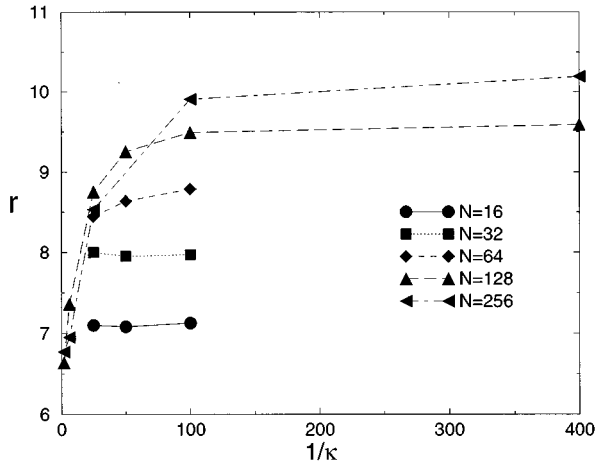

FIG. 2. $r=R_{\mathrm{end}}^2/R_G^2$ as a function of κ for $b=2$.

form straight blob poles. Furthermore a saturation is found. This kind of finite size effect will play an important role in the analysis of the bond angle correlation function (see Sec. V). Increasing the degree of polymerization from low values leads to stronger stretching as the mean energy per monomer increases. When N is large enough, the effects of screening show up, leading to a reduction of r. For infinitely large N (and finite r_D) all systems converge towards the SAW value around 6.3. As Fig. 3 shows, the crossover region is strongly dependent on b and κ.

The electrostatic persistence length L_P is the main target of our analysis. First we take a direct route to calculate L_P. R_{end} for a wormlike chain is given by [15]

$$R_{\mathrm{end}}^2=2LL_P-2L_P^2\left(1-\exp\frac{-L}{L_P}\right) \tag{3}$$

with $L=(N-1)b^2$ the contour length. Having L and R_{end}^2 L_P is determined numerically. The limiting behavior is that of a random walk and not of a self-avoiding walk. Therefore the SAW behavior shows that our chains are not exactly wormlike. Assuming the variational methods to be right, $L_P\kappa$ should be independent of κ while in the OSF case $L_P\kappa\sim 1/\kappa$. Plotting $L_P\kappa$ versus $1/\kappa$ leads to negatively

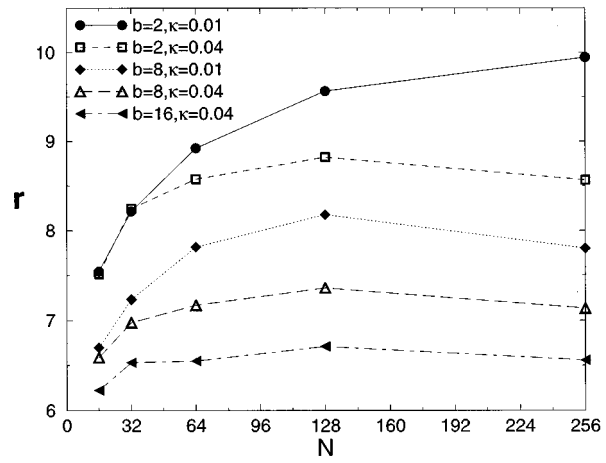

FIG. 3. $r=R_{\mathrm{end}}^2/R_G^2$ as a function of N.

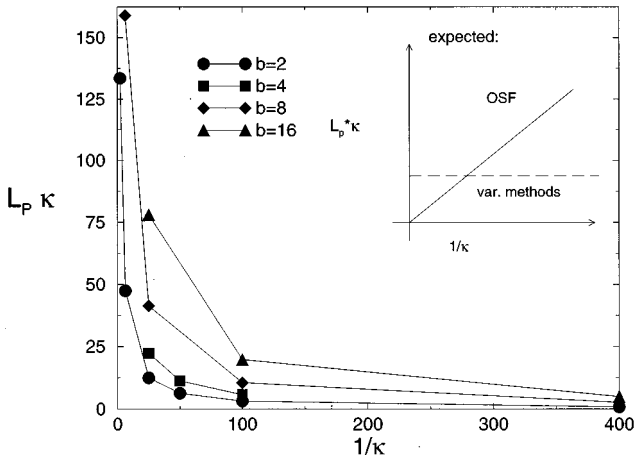

FIG. 4. $L_P\kappa$ vs $1/\kappa$ for $N=128$. The persistence length L_P is the numerical solution of the wormlike chain equation (3).

sloped curves meaning a sublinear $1/\kappa$ dependence of L_P (see Fig. 4). In spite of the fact that our chains are not exactly wormlike and of the finite size effects, this result is a clear hint that both theoretical predictions could be wrong for all relevant chain lengths.

Some theoretical approaches [13] use κb and λ_B/b as scaling parameter combinations. We checked the scaling of our data with κb (λ_B is fixed) aiming for a reduction of the effective dimension of our parameter space. As expected by looking at the explicit form of the Debye-Hückel potential no simple scaling can be figured out. Figure 5 demonstrates this for the simplest case.

IV. SCALING

In spite of the failure of these simple ''scaling'' attempts there should be a possibility to work out the scaling properties of our data, using the concept of electrostatic blobs [1]. In analogy to neutral polymers a blob is defined by the number of monomers g_e for which the total energy equals k_BT. As noticed in Sec. III, the bonds between the charges are stretched so that the assumption of unperturbed chains within the blobs has to be dropped. Nevertheless, this definition of

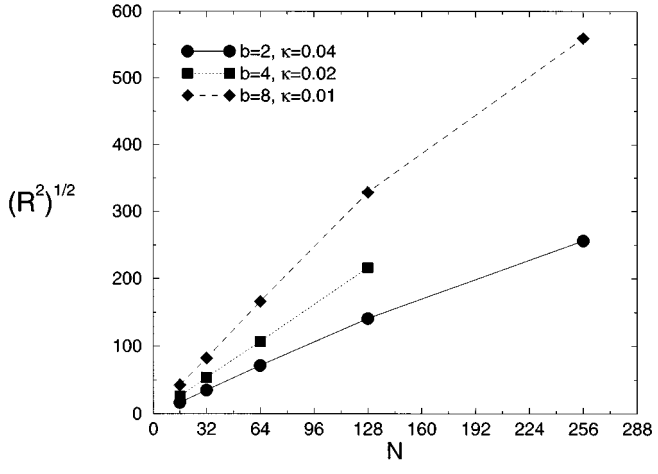

FIG. 5. End-to-end distance vs N for $b\kappa=$const.

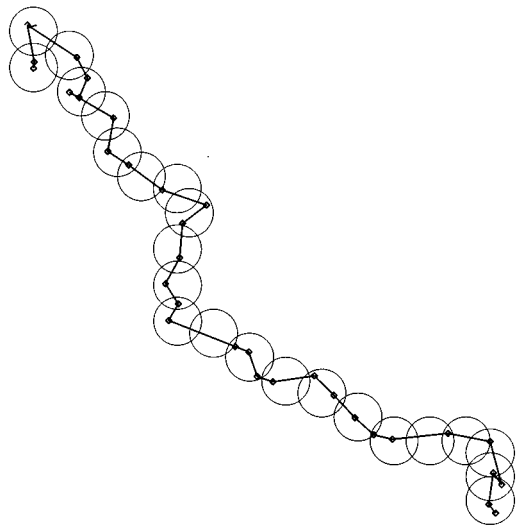

FIG. 6. Typical conformation of a blob pole with blobs indicated by circles ($N=32$, $b=2$, and $\kappa=0.04$). The projection is chosen to display the longest axis in the paper plane.

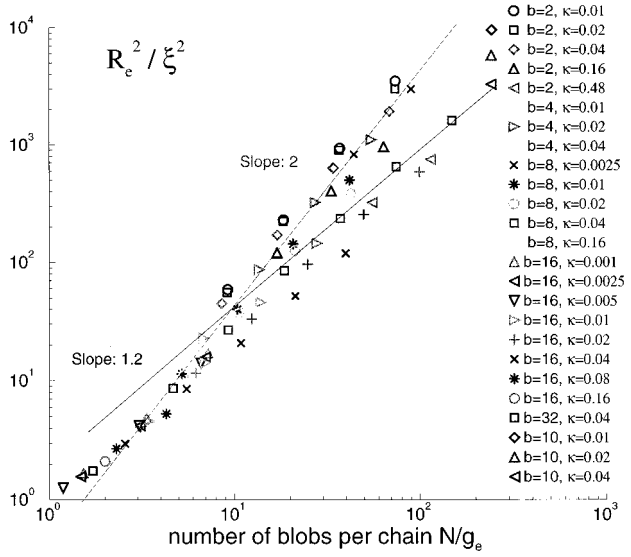

FIG. 7. R_{end}^2/ξ^2 as a function of L/ξ: No scaling of our data with ξ is found.

subunits of the chain is very useful.

First of all, the question of how to estimate the blob diameter ξ has to be settled. To avoid unnecessary assumptions (e.g., ideal chain statistic inside a blob) we calculated ξ from our data. The blob is defined by the number of monomers g_e for which the sum of electrostatic and bond stretching energy equals the thermal energy k_BT. Clearly, only the excess energy beyond the neutral elongation of the bond is taken into account. We restrict ourselves to central monomers to avoid artificial chain end effects. The knowledge of g_e and of the internal distances determines ξ. The κ dependence of both quantities is rather weak (slow decrease with decreasing κ), while the influence of the bond length is much stronger.

The meaning of these blobs is less profound as for neutral monomers, especially due to the loss of ideal chain statistics. Nevertheless, this kind of ''κ-dependent coarse graining'' is physically well motivated and strongly recommended by our configurations (see Fig. 6).

From neutral chains one would expect a scaling of the chain radii with ξ. This, however, does not work out here as Fig. 7 shows. Obviously the persistence length L_P is not a simple linear function of ξ. Remembering that the persistence length defines a kind of stiff chain segment length the chain dimensions should show a characteristic dependency on L_P. Therefore one should investigate R_{end} plotting R_{end}^2/L_P^2 versus the number of persistence lengths per chain. Using the Odijk formula and a formula due to the variational ansatzes a direct comparison of the scaling properties of the two different theories is possible. All variational theories predict $L_e \sim 1/\kappa$. Explicitly for a blob picture Ha and Thirumalai gave [8]

$$L_e \sim \frac{g_e}{\kappa}\sqrt{\frac{\lambda_B}{\xi}}. \tag{4}$$

The OSF theory [3,4] predicts

$$L_e = \frac{\lambda_B}{4\kappa^2 A^2}, \tag{5}$$

where A is the distance between two charges along the contour of the chain. Khokhlov and Khatchaturian [5] claim that after averaging over the transversal fluctuations of the flexible chains the same formalism applies to this ''renormalized'' chain, which is represented by a chain of blobs. Therefore, within the framework of a blob picture they formulate for L_P explicitly:

$$L_e \sim \frac{\lambda_B g_e^2}{\kappa^2 \xi^2}. \tag{6}$$

This means that A is defined as $A \sim \xi/g_e$ since every blob consists of g_e charges, which have a mean distance of ξ (imagine two charges of strength g_e in the center of two adjacent blobs). The number of persistence lengths per chain is calculated as $N\xi/g_eL_P$. N/g_e is the number of blobs so that $N\xi/g_e$ is the contour length of the blob chain. This means that the quantity at the abscissa is the ratio of contour length to persistence length. The results for both theories are shown in Figs. 8 and 9. It is important to realize that the persistence length is the sum of the electrostatic part L_e and the intrinsic persistence length L_0:

$$L_P = L_e + L_0. \tag{7}$$

In the case of a blob picture $L_0 = \xi$. Using L_0 equal to unity, which is the intrinsic persistence length of the neutral chains between the charges, leads to scaling plots similar to the ones generated according to (4) and (5) with a little worse scaling in the SAW regime. Nevertheless the intrinsic part is of enormous importance. Omitting L_0 and using L_e only destroys the scaling in the SAW regime in the OSF case, while the variational scaling holds quite well for our parameters. This accounts from the fact that in these cases the inequality

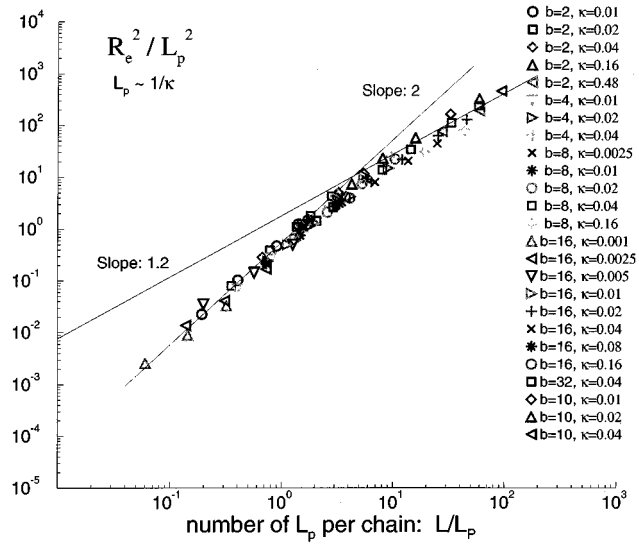

FIG. 8. Scaling plot due to the variational ansatzes: R^2_{end}/L_P^2 vs L/L_P. L/L_P is the number of persistence lengths per chain, $L_e \sim 1/\kappa$.

$L_{e,\mathrm{OSF}} \ll L_0$ holds, meaning that the electrostatic contribution is much smaller than the intrinsic persistence length while $L_{e,\mathrm{var}} \gtrsim L_0$.

From the first view it is clear that both theories show quite good scaling. There is no way to distinguish them. To explain this, it is necessary to divide the plot into two parts. For small X values the plots show straight lines with slope two. This is the regime where the chains build up blob poles. The dependence on L_P cancels out as is easily seen:

$$\frac{R_e^2}{L_P^2} \sim X^2 = \frac{N^2 \xi^2}{g_e^2 L_P^2} \Rightarrow R_e^2 \sim \frac{N^2}{g_e^2} \xi^2.$$

The end-to-end distance is proportional to the number of blobs times the blob diameter. For larger numbers of L_P per chain the behavior crosses over to a regime of slope 1.2. This is a SAW regime where the dependence on L_P is explicit:

$$\frac{R_e^2}{L_P^2} \sim X^{6/5} = \frac{N^{6/5} \xi^{6/5}}{g_e^{6/5} L_P^{6/5}} \Rightarrow R_e^2 \sim \left(\frac{N\xi}{g_e} \right)^{6/5} L_P^{4/5}.$$

Here something should be seen, but the κ dependence of R_e again seems to be so weak that no difference can be figured out. The scaling is dominated by the intrinsic part and is therefore more or less an N scaling. All in all, the fact that such an enormous amount of data collapses nicely over a lot of decades onto one curve, which describes very well the chain behavior from the blob pole in the case of weak screening up to the SAW regime, demonstrates that L_P is the relevant statistical segment length. As a central result of this chapter remains the demand to find a more sensitive quantity to measure the persistence length directly.

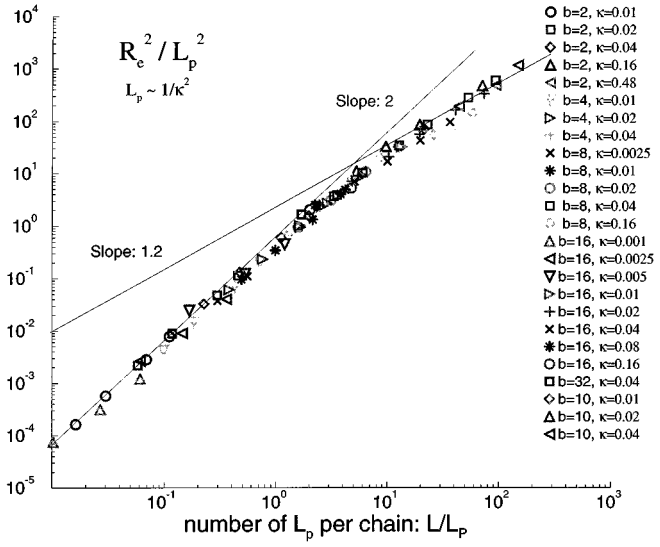

FIG. 9. Scaling plot due to the OSF approach: R^2_{end}/L_P^2 vs L/L_P. L/L_P is the number of persistence lengths per chain, $L_e \sim 1/\kappa^2$.

V. BOND ANGLE CORRELATION FUNCTION AND PERSISTENCE LENGTH

The most direct definition of L_P is simply geometrical [14]:

$$L_P = \frac{1}{2} \sum_{i=1}^{N/2-1} \langle \vec{b}_{N/2} \cdot \vec{b}_{N/2+i} + \vec{b}_{N/2} \cdot \vec{b}_{(N/2)-i} \rangle, \tag{8}$$

$\vec{b}_i$ again being the ith bond vector. In the case of exponentially decaying angular correlations, this approach is identical with the calculation of the bond angle correlation function (f_{BAC}). f_{BAC} can easily be formulated for a continuous model by comparing the normalized tangent vectors at t and $t+\Delta t$. In our bead spring model, f_{BAC} is defined via the scalar product of two normalized bond vectors:

$$f_{\mathrm{BAC}}(k) = \left\langle \frac{\vec{b}_j}{\|\vec{b}_j\|} \cdot \frac{\vec{b}_{j+k}}{\|\vec{b}_{j+k}\|} \right\rangle = \langle \cos[\phi(\vec{b}_j, \vec{b}_{j+k})] \rangle, \tag{9}$$

where $\phi(\vec{b}_j, \vec{b}_{j+k})$ is the angle between the two bond vectors and $\langle\ \rangle$ indicates the average over all polymers.

Since the persistence length is defined as the decay contour length of all angular correlations, f_{BAC} should show—after some ''transient time'' representing the inner part of the blob—an exponential decay, similar to a wormlike chain for which

$$f_{\mathrm{BAC}}(k) \sim \exp\left(-\frac{k}{L_P} \right) \tag{10}$$

applies, giving

$$B(k) = \ln\langle \cos\phi(\vec{b}_j, \vec{b}_{j+k}) \rangle \sim \ln \exp\left(-\frac{k}{L_P} \right) = -\frac{k}{L_P}. \tag{11}$$

To improve averaging, the reference point j is not fixed but moves along the chain. Clearly, this procedure leads to a big improvement for small and medium k while the effect is rather poor for large k because only few large distances are

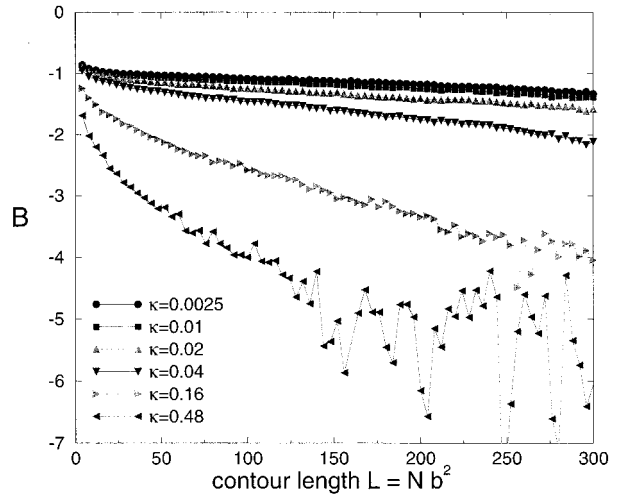

FIG. 10. Logarithm of the bond angle correlation function for $N=128$, $b=2$ and the specified κ values.

available. To avoid problems due to free ends, the outermost blobs are not taken into account (e.g., 20 monomers on each side for $N=128$). Another correlation function was defined by calculating the bond angle correlation function of the linking vectors between the centers of masses of the blobs. All these methods lead to the same results within the errorbars. Only data averaged with the first method are shown. Figures 10 and 11 show B for the system $N=128$, $b=2$ and $N=256$, $b=8$, respectively, at the specified κ values. The corresponding Tables I and II give the resulting persistence lengths and effective exponents y for subsequent κ values. All exponents are clearly smaller than one. In the $b=2$ case saturation is found. The exponent goes to zero for κ going to zero displaying strong finite size effects since the persistence lengths exceed the size of the chains. Therefore the ability of the chain to stretch is exhausted and the increase in L_P vanishes. To prove the validity of our arguments we have to compare these systems with larger chains. Figures 12 and 13 show two examples. There is an enormous difference for $b=2$ and $\kappa=0.01$, while the opposite extreme ($b=16$, $\kappa=0.04$) shows no finite size effects. Figure 13 points out that this bad κ value for $b=2$ works quite well for $b=8$, because the regarded chain is roughly a factor of 4 longer and therefore not influenced that strongly by finite size effects. It is obvious that this effect will show up in experiments as well.

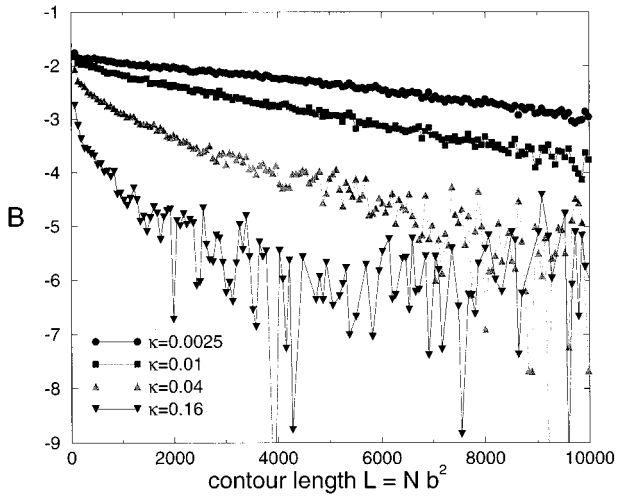

FIG. 11. Logarithm of the bond angle correlation function for $N=256$, $b=8$ and the specified κ-values.

TABLE I. Persistence lengths L_P and effective exponents y.

			$b=2$			
	$N=128$			$N=256$		
$1/\kappa$	L_P	L_P/L	y	L_P	L_P/L	y
400	948.6	1.853		2366.88	2.311	
			0.11			0.37
100	813.56	1.589		1418.44	1.385	
			0.32			
50	652.16	1.274		-		0.87
			0.78			
25	380.96	0.744		423.72	0.414	
			0.86			0.80
6.25	116.32	0.227		139.24	0.136	
			0.55			0.46
$2.08\overline{3}$	63.44	0.124		84.28	0.082	

All simulated systems were analyzed in this way and lead to the same answer. To figure out the influence of the bond stretching, we performed simulations with fixed bond lengths (see Sec. II). Additionally, we analyzed two-dimensional systems for both cases. The qualitative behavior is the same in all cases: The effective exponent of the κ dependence of the persistence length is continuously varying and smaller than 1 (see Fig. 14):

$$L_P \sim 1/\kappa^y; \quad y<1. \tag{12}$$

No unique power law can be derived, even if finite size effects and the statistical errors of the data are taken into account. Nevertheless, this puts the results of Secs. III and IV on a profound basis. But they are in strong contrast to all known analytical results. Recently, a new field theoretical approach was suggested pointing towards a sublinear behavior [16]. The common tendency with our data is encouraging, however, no mapping of the data was possible so far.

TABLE II. Persistence lengths L_P and effective exponents y.

			$b=8$			
	$N=128$			$N=256$		
$1/\kappa$	L_P	L_P/L	y	L_P	L_P/L	y
400	6508.16	0.794		8976	0.548	
			0.33			0.39
100	4114.56	0.502		5246.08	0.320	
			0.53			0.58
25	1954.56	0.239		2361.6	0.144	
			0.31			0.45
6.25	1276.8	0.156		1262.08	0.077	
						0.43
$2.08\overline{3}$				791.04	0.048	

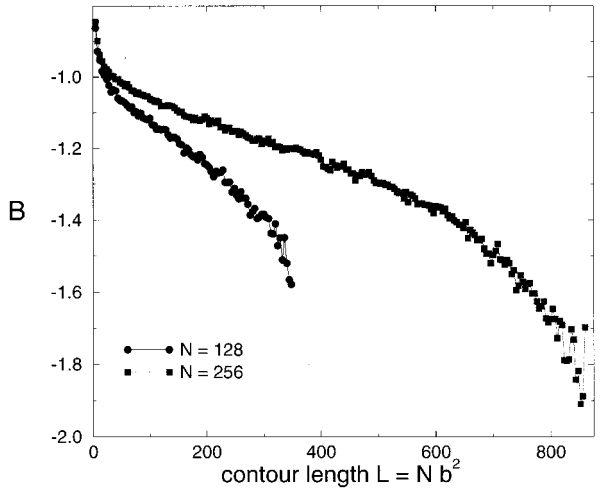

FIG. 12. Finite size effects on the logarithm of the bond angle correlation function: $b=2$ and $\kappa=0.01$.

VI. STRUCTURE FACTOR

To examine the chain conformation in detail at all length scales we calculate the spherically averaged structure factor $S(q)$. Additionally, the structure factor along the main axes of the gyration tensor of the chains is determined. The structure factor allows direct comparison to experimental data and is a necessary input for some theories [17,18].

$$S(q)=\left\langle \frac{1}{N}\left|\sum_{i<j}^{N}\exp[i\vec{q}\cdot(\vec{r}_i-\vec{r}_j)]\right|^2\right\rangle. \tag{13}$$

This formula demonstrates that $S(q)$ is the Fourier transform of the pair correlation function. The restriction to a certain direction means a restriction of $\vec{q}$ to this direction.

The scaling of $S(q)$ is predicted in analogy to the neutral case, where $S_{\text{neutral}}(q)$ scales as $q^{-1/\nu}$, ν being the exponent of the N dependence of the chain radii (e.g., $\nu=0.5$ for ideal chains and roughly 0.59 in good solvent). The range of validity is determined by the extensions of the polymer:

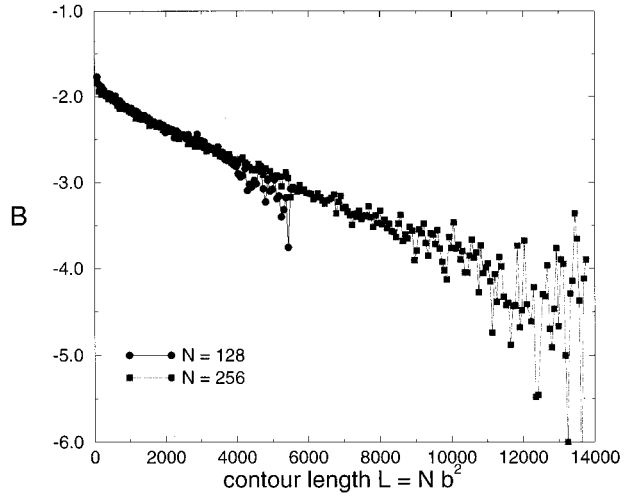

FIG. 13. Finite size effects on the logarithm of the bond angle correlation function: $b=8$ and $\kappa=0.01$.

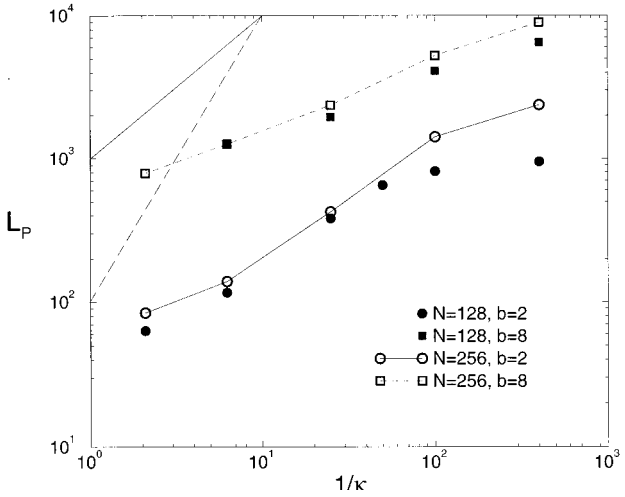

FIG. 14. Persistence length based on B vs $1/\kappa$. The two lines in the upper left corner indicate the slopes predicted by OSF (dashed) and the variational methods (solid). The model system should give the best description for weakly charged polyelectrolytes and therefore the upper curves.

$$\frac{2\pi}{R_{\text{end}}}\ll q\ll\frac{2\pi}{b}.$$

Viewing the polyelectrolytes as composed of rodlike segments of length L_P, which form an ideal chain, the scaling is expected to have the following form:

$$S(q)\sim q^{-2}\ \text{ for } q\ll\frac{2\pi}{L_P} \tag{14}$$

and

$$S(q)\sim q^{-1}\ \text{ for } q\gg\frac{2\pi}{L_P}. \tag{15}$$

Therefore the q value at the crossover can be used to calculate a measure for the persistence length.

First of all, the N dependence of $S(q)$ is examined to determine possible finite size effects. Figure 15 demonstrates

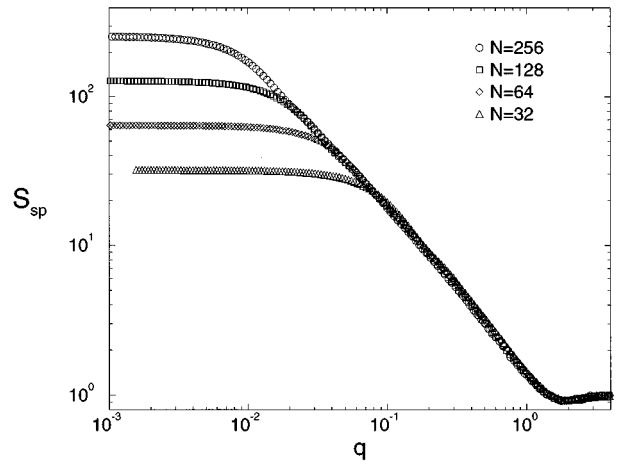

FIG. 15. Finite size effects on the structure factor for $b=2$ and $\kappa=0.01$.

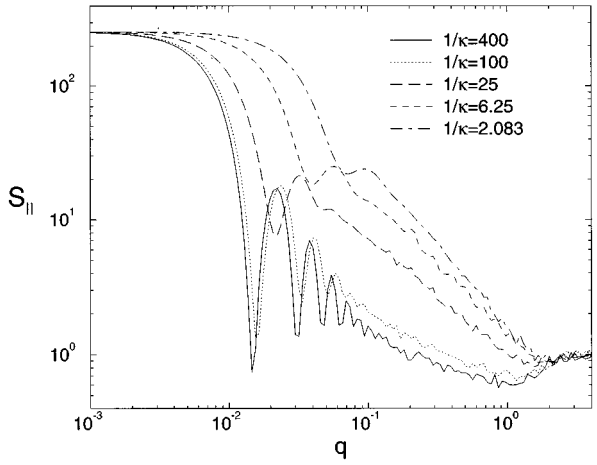

FIG. 16. Structure factor parallel to the first main axis of gyration for $N=256$ and $b=2$.

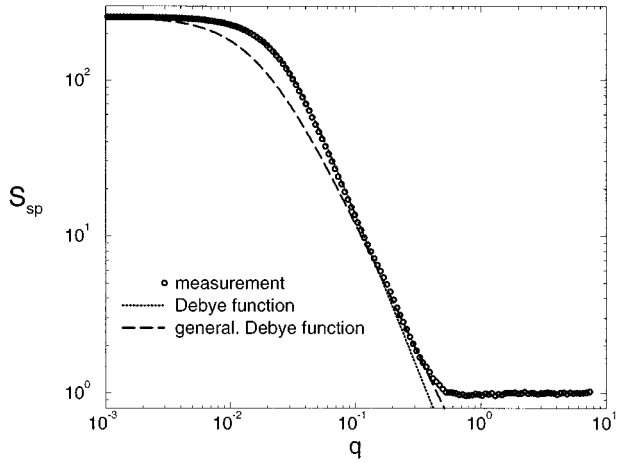

FIG. 17. Spherically averaged structure factor and fits for $N=256$, $b=8$, and $\kappa=0.48$.

that the finite size effects on $S(q)$ are relatively weak, since all curves deviate from the $N=256$ line only roughly at $q\approx 2\pi/R_{\mathrm{end}}$.

Looking first at the spherically averaged quantity shows that the logarithmic slopes seem to vary continuously between one (κ very small, $b=2$) and two (κ very large, $b=16$). As expected, the chains get stiffer with decreasing κ, leading to smaller slopes. This is consistent with the picture of the blob pole coming from scaling. To make this point even clearer, a plot of the structure factor parallel to the first main axis $S_{\|}$(q) is given. In the low-q regime pronounced oscillations are recognized (see Fig. 16). Such oscillations are expected for a rigid rod of which the structure factor is given by

$$S_{\mathrm{rod}}(q)=\frac{1}{N}\,\frac{1-\cos(Nbq)}{1-\cos(bq)}. \tag{16}$$

The first minimum is located at $q_{\mathrm{rod}}=2\pi/R_{\mathrm{end}}=2\pi/Nb$. This dependence is reflected by our data. The first minimum is especially for strong interacting systems given by R_{end}. Clearly, increasing κ leads to a shifting and a smearing out of these oscillations.

The analysis of the component perpendicular to the first main axis $S_{\perp}(q)$ is much more difficult. The elongation of the chain is rather small in this direction limiting the q interval of interest. Due to statistical fluctuations, it is difficult to determine very precise values, but the tendency is clear: The exponent is a function of b and κ and varies in the range $0.58<\nu<0.8$. All in all, the behavior of $S_{\perp}(q)$ is similar to the spherical averaged quantity in the high-q regime. Similar ν values were actually found in simulations of strongly charged polyelectrolytes [10].

The spherically averaged structure factor shows a kink between two regimes of different slopes. The low-q part is well fitted with a Debye function (which is expected at least in the Guinier region). The high-q regime can be described by a generalized Debye function as has been used successfully for strongly charged polyelectrolytes [10]:

$$S_{GD}(q)=\frac{N}{1+(qf)^{1/\nu_D}}, \tag{17}$$

where f and ν_D are fitting parameters. In the case of an ideal chain f equals $R_G/\sqrt{2}$ and $\nu_D=0.5$. For our systems f is roughly R_G and ν_D varies between 0.59 and 0.92. Again the variation over the whole conformational range from a SAW to an almost rodlike chain is reflected by these exponents (see Figs. 17 and 18).

The kink can, for instance, be identified by the crossing point of the two fitting functions. Using this q value to calculate a measure of the persistence length L_P leads to results that agree qualitatively very well with the values of the bond angle correlation function (see Fig. 19 and Table III). Again, the sublinear $1/\kappa$ dependence is recovered. This result is in strong contrast to simulations that take the counterions explicitly into account where a $1/\kappa$ dependence was suggested by the data [10].

If we had taken the neutral monomers between the charges into account, we would have found a nontrivial extension of the structure factor to higher q values. Remember-

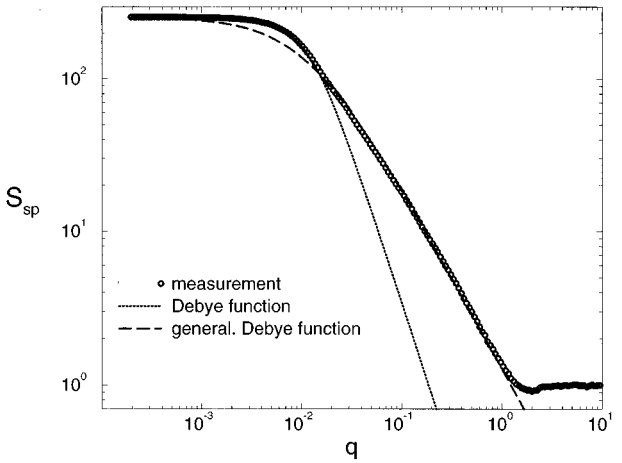

FIG. 18. Spherically averaged structure factor and fits for $N=256$, $b=2$, and $\kappa=0.0025$.

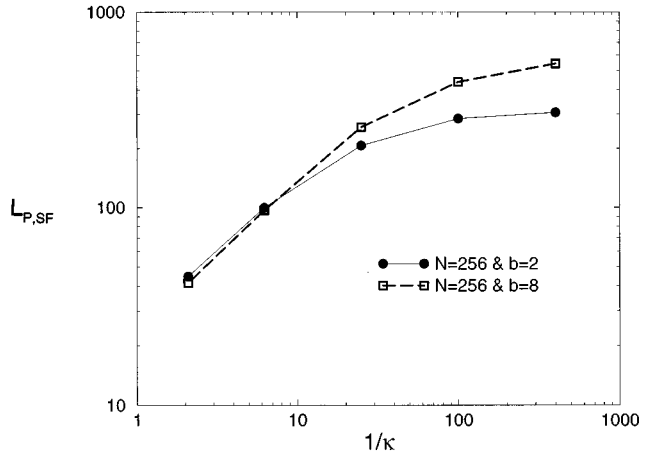

FIG. 19. Persistence length based on the crossing of the fitting functions vs $1/\kappa$. As the q values measure direct distances in space and not along the contour of the chain the absolute values differ from those resulting from the bond angle correlation. For quantitative comparison, the values have to be scaled by the bond length b. This would not lead to new information as the essential sublinear behavior will not be affected by this transformation.

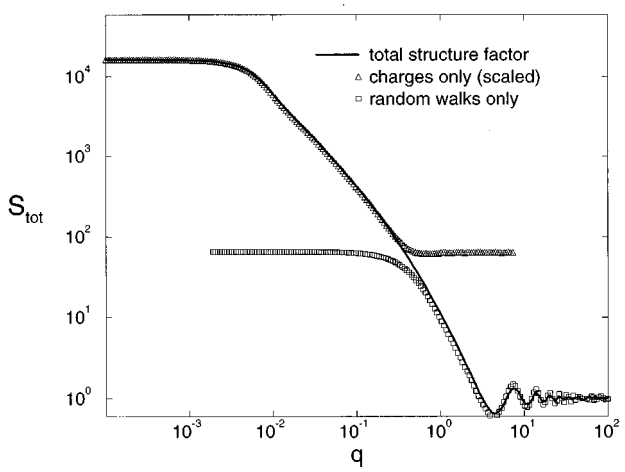

FIG. 20. Structure factor extended by introduction of neutral monomers compared to the structure factor of the charges only and to a Debye function for $N=256$, $b=8$, and $\kappa=0.01$.

ing that our bonds represent random walks and knowing the structure factor of a random walk to be a Debye function, we are able to extend the calculated structure factor of our polyelectrolyte chains to higher q values by introducing the Debye function into the plot. The measured $S(q)$ and the Debye function leave only a small gap that can be smoothly continued to give one curve. The gap is due to the pair correlation of monomers of different random walks which is inevitable in this easy approach. By introducing ideal neutral chains of step width one, b^2 steps, and accurate end-to-end distance and calculating the structure factor of this system, the validity of this simple approach is proven as Fig. 20 demonstrates.

All in all, the calculation of the structure factor reproduces only the roughest features of the scaling picture (kink at L_P separates two regimes of different slopes). Unfortunately, it resists fitting any detailed theoretical descriptions. All conclusions of the former sections are verified. Especially the results on the persistence length are recovered, impressively showing the overall consistency of the present analysis.

TABLE III. Persistence lengths L_P and effective exponents y from structure factor

	$N=256$			
	$b=2$		$b=8$	
$1/\kappa$	L_P	y	L_P	y
400	305.45		543.53	
		0.05		0.16
100	284.82		437.58	
		0.23		0.38
25	207.09		257.61	
		0.53		0.71
6.25	99.94		96.84	
		0.73		0.77
$2.08\overline{3}$	44.79		41.54	

VII. CONCLUSIONS

The behavior of single, intrinsically flexible, weakly charged polyelectrolyte chains is examined by extensive numerical simulations. Varying κ, b, and N the whole relevant parameter space can be covered. κ-dependent chain stretching on both short and long length scales is reported. The scaling plots of Sec. IV demonstrate the crossover from a blob pole to a self-avoiding walk regime.

In order to clarify the question whether the OSF theory is extendable to intrinsically flexible polyelectrolytes [5,6], we focused on the calculation of the electrostatic persistence length, because this quantity is given explicitly by all theoretical approaches. Using several different methods, we always end up with the same result: The persistence length depends in a sublinear way on $1/\kappa$ without showing a clear unique power law:

$$L_P \sim \frac{1}{\kappa^y}, \quad y<1.$$

This is in strong contrast to the analytical predictions, which favor $1/\kappa^2$ (OSF [3,4]) or $1/\kappa$ (variational methods [7–9]). Although some systems are influenced by strong finite size effects, which will be relevant even for experimental systems but are controllable in computer simulations, this result is unequivocal. A $1/\kappa^2$ dependence can definitively be excluded. There exists no hint for a convergence towards a $1/\kappa$ behavior in our data, although we choose the smallest Debye radius smaller than the smallest bond length and the biggest larger than the whole chain. Unfortunately, no clear power law with a well-defined exponent shows up. The exponent itself seems to depend on b and κ for all relevant chain lengths : $y=y(\kappa,b)$. Especially the structure factor calculations strongly support these results.

Recently, a sublinear dependence of L_P with respect to $1/\kappa$ was suggested by a new field theoretical, variational approach [16]. The qualitative agreement of this solution with our data is an encouraging sign. It can be concluded from our simulations that the stiffness of intrinsically flexible polyelectrolyte chains is much less influenced by the screening

parameter as expected. For that the fraction of charges (equivalent to $1/b^2$) plays an important role, too, since it determines the entropy. It is obvious from our data that the entropic part of the free energy is underestimated by all known analytical approaches for (at least) all relevant chain lengths. While most large scale properties are well understood by simple arguments, there exists a lack of detailed understanding, as is demonstrated at the example of the electrostatic persistence length. An interesting challenge for future work on this topic should be the variation of the intrinsic persistence length to study the crossover from the OSF regime, where the intrinsic persistence length is dominating, to the regime of extremely flexible chains described by our data.

ACKNOWLEDGMENTS

We would like to acknowledge stimulating discussions with M. Stevens, J.F. Joanny, A. Liu, P. Pincus, and especially R. Everaers. A large grant of computer time at the HLRZ Jülich, Germany, is gratefully acknowledged.

[1] P. de Gennes, *Scaling Concepts in Polymer Physics* (Cornell University Press, Ithaca, NY, 1979).
[2] K. Kremer, B. Dünweg and M. Stevens, in *Monte Carlo and Molecular Dynamics Simulation in Polymer Science*, edited by K. Binder (Oxford University Press, Oxford, 1995).
[3] T. Odijk, J. Polym. Sci. Polym. Phys. Ed. **15**, 477 (1977).
[4] J. Skolnick and M. Fixman, Macromolecules **10**, 944 (1977).
[5] A. R. Khokhlov and K. A. Katchaturian, Polymer **23**, 1742 (1982).
[6] H. Li and T. Witten, Macromolecules **28**, 5921 (1995).
[7] J.-L. Barrat and J.-F. Joanny, Europhys. Lett. **24**, 333 (1993).
[8] B.-Y. Ha and D. Thirumalai, Macromolecules **28**, 577 (1995).
[9] D. Bratko and K. A. Dawson, J. Chem. Phys. **99**, 5352 (1993).
[10] M. Stevens and K. Kremer, J. Chem. Phys. **103**, 1669 (1995) [see additionally M. Stevens and K. Kremer, Phys. Rev. Lett. **71**, 2228 (1993); Macromolecules **26**, 4717 (1993)].
[11] K. Kremer and G. Grest, Phys. Rev. A **33**, 3628 (1986).
[12] J.-L. Barrat and J.-F. Joanny (private communication).
[13] J.-L. Barrat and D. Boyer, J. Phys. (France) II **3**, 343 (1993).
[14] G. A. Christos and S. L. Carnie, J. Chem. Phys. **91**, 439 (1989).
[15] M. Doi and S. F. Edwards, *The Theory of Polymer Dynamics* (Oxford University Press, Oxford, 1986).
[16] A. J. Liu, J. Rudnick, and A. Levine (unpublished).
[17] J. M. Victor, J. Chem. Phys. **95**, 600 (1991).
[18] T. A. Vilgis and R. Borsali, Phys. Rev. A **43**, 6857 (1991).